

Equation of state and critical exponents of ^3He and a ^3He - ^4He mixture near their liquid-vapor critical point*

Charles Pittman, Theodore Doiron,[†] and Horst Meyer

Department of Physics, Duke University, Durham, North Carolina 27706

(Received 21 May 1979)

We report a determination of the effective critical exponents β_{eff} and γ_{eff} in ^3He as a function of the distance $T - T_c$ from the liquid-vapor critical point. These exponents characterize respectively the singular behavior of the densities for the coexisting phases ($T < T_c$) and of the compressibility along the critical isochore for $T > T_c$. The density measurements use the dielectric-constant method and cover the range $2 \times 10^{-1} > |t| > 3 \times 10^{-5}$ where $t = (T - T_c)/T_c$. Far away from T_c we find $\beta_{\text{eff}} = 0.36$, but as T_c is approached, β_{eff} decreases progressively. Although the error becomes large for $t \leq 5 \times 10^{-4}$, β_{eff} tends into the direction of the limiting value $\beta = 0.32$ that is predicted by recent theories. For $2 \times 10^{-2} > t > 5 \times 10^{-4}$, we find $\gamma_{\text{eff}} = 1.19 \pm 0.01$. Both the coexistence curve and the compressibility are fitted to power-law series that include correction-to-scaling terms. The amplitudes of these terms for the coexistence curve are compared with those for Xe and SF_6 . The slope of the rectilinear diameter is found to be $d\rho/\rho_c dt = -0.022$. For the 80%- ^3He -20%- ^4He mixture above T_c , the singular density gradient in the earth's gravity field is found to diverge strongly as T_c is approached. The relevant exponent is again $\gamma_{\text{eff}} \approx 1.18 \pm 0.02$ and the amplitude of the singular term is intermediate between those for ^3He and for ^4He . These results are in good agreement with those calculated from the Leung-Griffiths model for ^3He - ^4He mixtures.

I. INTRODUCTION

It has been known for several years that the effective critical exponents γ_{eff} and β_{eff} for pure ^3He and ^4He near the liquid-vapor critical point, measured for $|t| = |(T - T_c)/T_c| > 10^{-4}$,¹⁻⁵ differ from the asymptotic exponents for CO_2 , SF_6 , and Xe determined still closer to T_c .⁶⁻⁸ These exponents are defined by

$$\beta_{\text{eff}} = \frac{d \ln |\Delta\rho|}{d \ln |t|}, \quad T \leq T_c, \quad (1a)$$

$$\gamma_{\text{eff}} = -\frac{d \ln (\partial\rho/\partial P)_T}{d \ln t}, \quad \rho = \rho_c, \quad T \geq T_c, \quad (1b)$$

where $\Delta\rho \equiv (\rho_c - \rho_{L,V})/\rho_c$, and where ρ_L , ρ_V , and ρ_c are, respectively, the number densities for the coexisting liquid and vapor phases and at the critical point. Also $(\partial\rho/\partial P)_T \rho^{-1} \equiv k_T$ is the compressibility in the one-phase region. From the universality principle, one expects the asymptotic value of β_{eff} and γ_{eff} to be the same for all the simple fluids. Table I presents a review of the values for the two exponents as determined¹⁻¹¹ for ^3He , ^4He , and Xe and also the limiting values very close to T_c as predicted from renormalization-group (RG) theory and series expansion for the lattice gas.¹² In the earlier experiments T_c was often determined assuming a simple power law for the coexistence and compressibility singularities over a range up to about $|t| = 10^{-2}$. The recent observations^{6-8,11,13} that this assumption is not valid

for pure fluids shows the importance of the exact location of T_c and the need for better experiments with the He isotopes.

The purpose of the present paper is to describe a new determination of the densities ρ_L and ρ_V and k_T as a function of $|T - T_c|$ for ^3He over a larger temperature range than before. Particular emphasis was put on the best possible determination of T_c from the data in the immediate proximity of the critical point, in order to permit an improved analysis of the critical singularities. The method used the measurement of the dielectric constant and we believe this to be the largest collection of such data for ^3He , spanning approximately four decades for $T < T_c$. From their analysis, we determine first T_c and then β_{eff} and γ_{eff} as a function of $|t|$.

Furthermore using the same method, we report results on the vertical density gradient for an 80%- ^3He -20%- ^4He mixture near the liquid-vapor critical point as a function of t along the critical isochore. We demonstrate experimentally its predicted strong divergence based on the theory by Griffiths and Wheeler¹⁴ and compare the results with calculations from the Leung-Griffiths model.¹⁵

In Sec. II, we describe the experimental method and the procedures; Sec. III contains the presentation of the results, their analysis, and the comparison with results in other fluids. Finally, Sec. III describes the vertical-density-gradient measurements in the 80%- ^3He -20%- ^4He mixture and compares the results with the predictions.

TABLE I. Critical exponents and amplitudes for the normalized compressibility $P_c \rho_c^{-2} (\partial \rho / \partial \mu)_T = \Gamma^+ t^{-\gamma_{\text{eff}}}$ above T_c and the normalized coexistence curve $(\rho_L - \rho_V) / \rho_c = B |t|^{\beta_{\text{eff}}}$ for ^3He , ^4He , Xe, and the lattice-gas model. The symbol a represents the slope for the rectilinear diameter.

Fluid Expt.	Ref.	γ_{eff}	Γ^+	Range in $ t $	β_{eff}	B	Range in $ t $	T_c (K)	a
^4He	1	1.17 ± 0.0005	0.161	$< 2 \times 10^{-2}$	0.355 ± 0.003	1.40	$4 \times 10^{-5} \leftrightarrow 2 \times 10^{-1}$	5.190	...
^3He	2	1.18 ± 0.04	0.213	$6 \times 10^{-4} \leftrightarrow 4.5 \times 10^{-2}$	0.361 ± 0.005	1.31	$1.5 \times 10^{-4} \leftrightarrow 3 \times 10^{-1}$	3.310	-0.01
	3	1.19 ± 0.03	0.20	$1.5 \times 10^{-3} \leftrightarrow 3 \times 10^{-2}$	0.365 ± 0.005	1.33	$1 \times 10^{-4} \leftrightarrow 3 \times 10^{-1}$	3.309	-0.04
	4	1.14 ± 0.05	...	$10^{-3} \leftrightarrow 3 \times 10^{-2}$					
	5	1.16 ± 0.02	0.22	$4 \times 10^{-4} \leftrightarrow 6 \times 10^{-3}$				3.309	
Xe	6	1.23		$5 \times 10^{-6} \leftrightarrow 5 \times 10^{-5}$	0.329	1.48	$5 \times 10^{-5} \leftrightarrow 5 \times 10^{-5}$	289.71	
	7				0.317 ± 0.004	1.31	$3 \times 10^{-6} \leftrightarrow 4 \times 10^{-5}$		
	9	1.21	0.0676		0.356 ± 0.002	1.83	$2 \times 10^{-5} \leftrightarrow 3 \times 10^{-2}$	289.79	0.691
	10								0.73
	11	1.260 ± 0.02	0.056	$3 \times 10^{-5} \leftrightarrow 4 \times 10^{-2}$	0.337 ± 0.003	1.65	$1 \times 10^{-5} \leftrightarrow 10^{-3}$	289.76	
Theory									
Lattice gas	12								
Series expansion		1.250 ± 0.003			0.312 ± 0.005				
RG		1.241 ± 0.002							
RG (perturbative series)		1.2401 ± 0.0009			0.320 ± 0.015				
					0.325 ± 0.001				

II. EXPERIMENTAL

A. General considerations

In our experiment, the number density of the fluid is determined from the dielectric constant ϵ using the Clausius-Mossotti relation¹⁶ where the polarizabilities p of both He isotopes are the same within experimental error, about 0.1%.¹⁷ Even though p is only $0.0123 \text{ cm}^3/\text{mole}$,¹⁷ standard capacitance techniques permit a resolution of $\delta\rho/\rho \approx 10^{-6}$ which is adequate for the measurements both above and below the critical point. Recent measurements¹⁷ have shown furthermore that p is only weakly dependent on density and any singular behavior of ϵ at constant volume near T_c is so small as to be unobservable.¹⁸ Hence the method using the dielectric constant appears to be ideal for both the He isotopes, since a change in ϵ will correspond to a change in ρ alone.

Briefly, the method consists in measuring the capacitance of two horizontal superposed capacitors, the gaps of which are separated by approximately $\delta h = 2 \text{ mm}$. The capacitors are connected to a ratio-transformer bridge in such a way as to compare the top capacitance with the bottom one, or with a very

stable reference capacitor in thermal contact with the measuring cell. Therefore, one can obtain the difference in the dielectric constants, $\epsilon_{\text{TOP}} - \epsilon_{\text{BOTTOM}}$, and ϵ_{TOP} , respectively, henceforth labeled ϵ_T and ϵ_B .

At temperatures *below* T_c and under conditions where the liquid-vapor meniscus is situated between the two capacitors, the density of each phase can be measured, namely, ϵ_T and ϵ_B lead to ρ_V and ρ_L , respectively. *Above* T_c , the difference $\epsilon_B - \epsilon_T$ gives the density change $\delta\rho$ over the height δh . Assuming for the moment that the density gradient $\delta\rho/\delta z$ is constant over the cell height, and noting that for a pure fluid, the chemical potential change $\delta\mu$ in the gravity field is given by

$$\delta\mu = \rho g m \delta z, \quad (2)$$

where m is the molecular mass and g is the gravitational constant, we obtain $\delta\rho/\delta\mu = (\partial\rho/\partial\mu)_T = \rho^2 k_T$. In practice however, the large values of k_T near T_c produce significant deviations from a constant density gradient.^{19,20} Also there will be differences between the densities at the meniscus below T_c and those recorded by the two capacitors. Hence the actual measurements only reproduce approximately the coexistence curve as T_c is approached very closely.

In fact, for the He isotopes, these effects are particularly severe²⁰ and introduce by far the greatest uncertainty in the analysis of the results. As we shall see, gravity effects in ³He will limit a reliable determination of the coexistence curve to $-t > 3 \times 10^{-5}$ and the compressibility at $\rho = \rho_c$ to $t > 5 \times 10^{-4}$.

In a ³He-⁴He mixture, the density gradient $(\delta\rho/\delta z)_T$ above T_c is shown to be the sum of two terms proportional, respectively, to the compressibility at constant chemical potential, $k_{T,\Delta}$, and to the concentration susceptibility $(\partial X/\partial\Delta)_{T,P}$. Both quantities diverge strongly as T_c is approached and are related by simple thermodynamics. Hence measurements of $(\delta\rho/\delta z)_T$ should show a strong divergence. Therefore, similarly to the pure fluids, there will be deviations from a constant vertical density gradient sufficiently close to T_c .

Capacitive determinations of $(\partial\rho/\partial\mu)_T$ based on the vertical density profile were already made by Weber²¹ for O₂. In that experiment, however, six superposed capacitors were used, spanning a total height of about 12 cm. Measurements of $(\partial X/\partial\Delta)_T$ for ³He-⁴He mixtures along the critical line²² of the superfluid transition were also carried out with the same method and using the same double-capacitor cell as in the research to be described.

B. Capacitor cell

Because the capacitance cell has already been discussed in Ref. 22, only a brief description is given here. There are two horizontal capacitors made of perforated stainless-steel foils, mounted one on top of the other and spaced in height by 1.93 mm. Preliminary design estimations showed that this separation was a reasonable compromise between the requirements for good sensitivity in the measurement of $(\partial\rho/\partial\mu)_T$, for sampling the density over a small enough height to minimize problems very close to T_c , and for providing an acceptable mechanical rigidity of the plate system. The purpose of using perforated foils was to shorten the time for the establishment of equilibrium in the fluid near T_c , in particular for the ³He-⁴He mixture where the isotopes have to diffuse through the fluid sample to establish the equilibrium vertical concentration gradient. A stainless-steel capillary of ~ 0.15 -mm inner diameter connected the sample cell with the gas supply system at room temperature. The cell was thermally attached to a platform cooled by pumping on a bath of ⁴He, the temperature of which could be regulated to within approximately 1 μ K. Attached to this platform were also a reference capacitor, C_S , with two leads, encased in a copper container, and a ⁴He vapor pressure bulb. The five coaxial lines to the three capacitors were then electrically connected to a switch leading to a ratio transformer bridge as described previously.²³

All three capacitances in the cryostat were designed so as to have approximately the same value, and the measured capacitance ratios

$$R_{TS} = \frac{C_T}{C_T + C_S} \quad \text{and} \quad R_{TB} = \frac{C_T}{C_T + C_B} \quad (3)$$

were then close to 0.5. This matching had the advantage in reducing any differential thermal effects on the lead impedance during the periodic refilling of the cryostat with cryogenic fluids.

C. Experimental procedure

First, the effect of pressure on the capacitors C_T and C_B was determined at 77 K by measuring R_{TS} and R_{TB} as a function of density of ³He gas. Second, the thermometers were calibrated by means of the vapor pressure of ³He and ⁴He using the T_{58} and T_{62} scales, respectively, and the ratios R_{TS} and R_{TB} of the empty capacitors were measured against temperature between 2.8 and 3.8 K. The high-purity ³He (less than 50 ppm ⁴He) was then introduced at a temperature above T_c and its density adjusted to a value close to ρ_c . After filling, the valve on the top of the cryostat leading to the cell was closed. It was estimated that the amount of sample in the capillary was then less than 0.5% of the sample in the cell. The density variations in the cell caused by temperature changes in the capillary during one experiment were then calculated to be negligible and unlikely to affect the data. Alternating measurement of R_{TS} and R_{TB} were then taken at successive temperatures. The $R(T)$ data were processed, taking into account the corrections due to pressure deformation, $\delta R_P(T)$, and due to the temperature dependence of the empty capacitor, $\delta R_0(T)$. From the corrected ratio $R_{\text{corr}}(T)$, given by

$$R_{\text{corr}}(T) = R(T) - \delta R_P(T) - \delta R_0(T) \quad (4)$$

the absolute value of the dielectric constant ϵ_T or the difference $\epsilon_T - \epsilon_B$ were obtained via the Clausius-Mossotti relation. The value $p(\rho_c) = 0.1234$ cm³/mole was used,¹⁷ a small correction being made for the density dependence of p . It must be pointed out that in practice, this method can only detect the temperature-dependent term of $\epsilon_T - \epsilon_B$. A constant background term is normalized to zero because it is undistinguishable from any other apparatus effect.

The times to reach equilibrium were approximately 5 min far above T_c , but increased to several hours in proximity of T_c . In the two-phase region, the times were appreciably longer than those above T_c , which is consistent with previous observations during calorimetric measurements.²⁴⁻²⁶ After completion of the measurements for one given average fluid density $\bar{\rho}$, a small amount of fluid was removed from the cell

at a temperature well above T_c and a new series of measurements were carried out. In this way, the dielectric constant at about nine densities $1.03 \geq \rho/\rho_c \geq 0.97$ was determined.

The rationale for this apparent duplication of data was based on the need to establish the critical temperature with the smallest possible uncertainty. Our initial attempts were to measure the coexistence curve extremely close to T_c by rapidly cooling the fluid at the critical density from a temperature above T_c . This "quenching" method was to permit the two phases to form but without the time for the establishment of the density gradient within each phase, and it was to permit measuring the coexistence curve free from gravity-caused density gradients. However, unlike in the room-temperature experiments with Xe,⁷ this method failed. We were never able to see, on the chart plot of R_{TS} versus time, a clear separation between the regime in which temperature equilibrium and phase-separation were established, and the regime where the barometric density distribution was formed with a much longer time constant. The only measurements of R_{TS} and R_{TB} that were reproducible at a given t were those under conditions of complete equilibrium. Representative data for ρ_T and ρ_B close to T_c for $\bar{\rho} = \rho_c$ are shown in Fig. 1. The solid lines were calculated using the theory of Hohenberg and Barmatz.¹⁹ The parameters used here are listed in Table II, together with the relevant references. Clearly from the measurements at $\bar{\rho} = \rho_c$ alone, a determination of T_c with the required precision is out of the question. Hence measurements at slightly different densities $\bar{\rho}$ were carried out. Since the men-

iscus was then not situated in the middle of the cell, but its position was rapidly changing with t near T_c , it was possible to measure rather sharply the temperature and dielectric constant when the meniscus was starting and finishing to cross one of the capacitors. This is illustrated for $\bar{\rho}/\rho_c = 0.977$ in Fig. 2. Starting at $T > T_c$ and with decreasing temperature, the sharp minimum in ρ measured by the bottom capacitor at A indicates the first droplet of liquid between the plates, and therefore the arrival of the meniscus from below. As T decreases further, the meniscus crosses the capacitor and this passage is completed when a sharp kink at B signals the coexistence curve on the liquid side to be reached. Hence both the minimum and the kink represent points on the coexistence curve without substantial gravity effects. The density at $T < T_c$ measured by the top capacitor reflects gravity effects since now the distance to the meniscus is approximately 2 mm.

This procedure was repeated at a number of densities. As $|\bar{\rho} - \rho_c|/\rho_c$ decreased, the temperature difference between the sharp features gradually disappeared. For $|\bar{\rho} - \rho_c|/\rho_c \approx 0.025$ one curve measured by one of the capacitors then corresponded very closely to either ρ_V or ρ_L at the meniscus (see Fig. 2). An important check was the internal consistency between the location of A and B at the various average densities and the coexistence curve obtained from $|\bar{\rho} - \rho_c|/\rho_c \approx 0.025$.

After accumulation of a sufficient amount of data for ρ_L and ρ_V , the average density $\rho_L + \rho_V = 2\rho_d$ was obtained as a function of T , and the extrapolation to the vanishing difference $\rho_L - \rho_V$ gave the critical den-

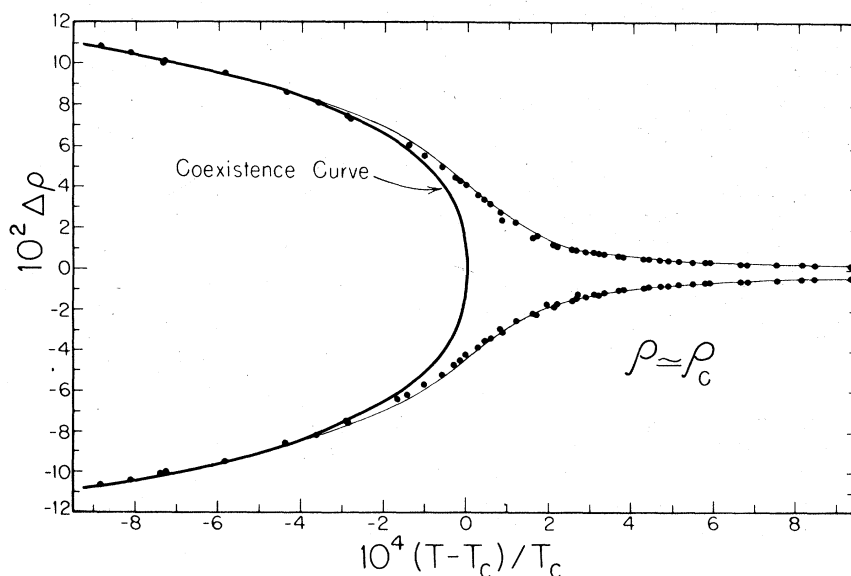


FIG. 1. Portion of the ρ_B and ρ_T density data, measured by the bottom and top capacitors as a function of reduced temperature $-t = -(T - T_c)/T_c$ for the density $\bar{\rho} = \rho_c$. The thin line represents the calculations for the vertical profile, using the linear model approximation (Ref. 19). The thick solid line is the calculated coexistence curve using the density data in Sec. III.

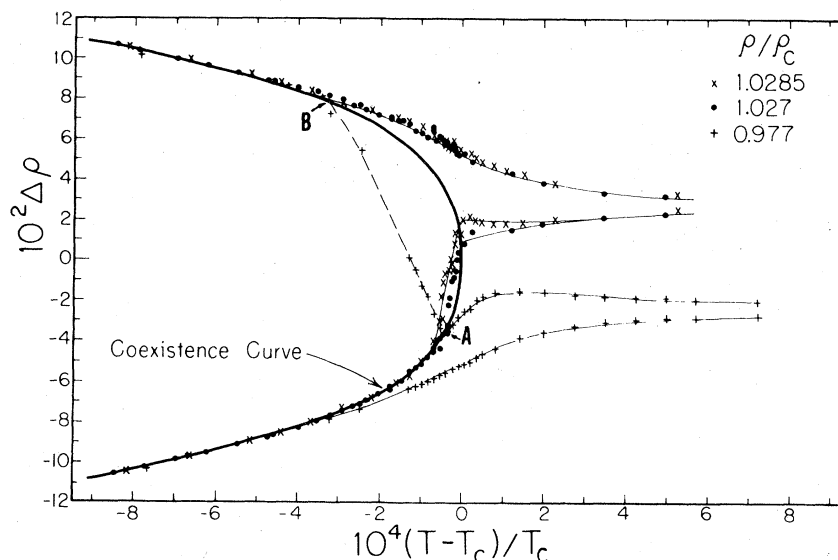


FIG. 2. Portion of the ρ_B and ρ_T density data for ^3He as a function of $-t$ for three representative densities. The sharp features *A* and *B* for the densities $\bar{\rho}/\rho_c = 1.0285$ and 0.977 indicate when the meniscus enters and leaves the bottom capacitor and hence provide points on the coexistence curve. The thick solid line is again the calculated coexistence curve using the density data in Sec. III. The thin solid lines and the dashed line are just a guide to the eye for the experimental data.

sity ρ_c . The location of T_c was obtained from a combination of several observations. First, we used the "kink" points described in connection with Fig. 2, that were closest to T_c . Furthermore using data for $(\bar{\rho} - \rho_c)/\rho_c \approx 0.025$ at $T_c - T < 100 \mu\text{K}$, we also plotted $\Delta\rho^{1/\beta}$ vs T for the coexistence curve. These data were least affected by gravity because the meniscus was located just below the top capacitor. The two reasonable choices for β were 0.32 and 0.34, the first one corresponding to the expected asymptotic exponent. By necessity, there were too few points to show which β came closest to giving a straight-line representation, but the temperature difference of the

TABLE II. Parameters used in the linear model calculation for the vertical density profile $(\partial\rho/\partial z)_T$ of fluid ^3He in the earth's gravity field. The parameter b^2 is calculated using the "minimization" condition quoted in Ref. 19. P_c is taken from Ref. 2. The choice of B and β is based on the data in the present work, but the calculated $(\partial\rho/\partial z)_T$ is rather insensitive to these values in the range $t > 3 \times 10^{-4}$.

$P_c = 0.1168 \text{ MPa} = 859.6 \text{ Torr}$	
$\rho_c = 0.01374 \text{ mole/cm}^3$	
$\Gamma = 0.209$	$\gamma = 1.19$
$B = 0.99$	$\beta = 0.32$
$b^2 = 1.286$	

intercept at $\Delta\rho = 0$ for both choices was only $20 \mu\text{K}$. Finally, the combination of the various observations located the critical temperature (^3He , 50-ppm ^4He) as

$$T_c = 3.3098 \text{ K} ,$$

where the uncertainties are estimated to be $\pm 30 \mu\text{K}$ relative to the other temperatures measured and $\pm 0.5 \text{ mK}$ on the absolute scale obtained using the ^4He vapor pressure calibration and the T_{58} tables.

This value of T_c was then used for the analysis of the $(\partial\rho/\partial\mu)_T$ above T_c . In order to determine with precision the background effects, δR_p and δR_0 , and to subtract them from the term δR_{grav} induced by the vertical fluid density change, ratio measurements were carried out up to $t \approx 10^{-1}$, where the latter was negligible. Because above T_c , $(\partial P/\partial T)_V$ for He is almost constant,⁶ δR_p varies linearly with T and can be distinguished easily from the effect caused by gravity. The temperature variation of the two terms δR_p and δR_{grav} became comparable for $t \sim 5 \times 10^{-2}$ and was much larger than the change of the empty capacitors, $\delta R_0(T)$.

In the ^3He - ^4He mixture, the determination of the exponent describing the divergence of $\rho_B - \rho_T$ above T_c was less accurate than for ^3He . Here the location of T_c was more difficult because of the very long times required to reach equilibrium below T_c .²⁴ The critical temperature determined from previous experiments for this same mixture^{27,28} was $T_c = 3.705 \pm 0.002 \text{ K}$, and was used as a first guide. The final value we adopted was 2 mK lower, as determined from a least-squares fit. Measurements of $\rho_B - \rho_T$

were carried out for several densities close to ρ_c . Model calculations, based on Ref. 15, show that at a given t , $\rho_B - \rho_T$ is maximum along the critical isochore, and indeed our experiments showed a flat maximum at $\bar{\rho} = 0.0144 \text{ cm}^{-3}$, which we had estimated to be very close to ρ_c .

III. RESULTS AND DISCUSSION

The density data below T_c for the ${}^3\text{He}$ coexisting liquid and vapor phases, and also $\rho_B - \rho_T$ above T_c for both ${}^3\text{He}$ and the ${}^3\text{He}$ - ${}^4\text{He}$ mixture have been tabulated²⁹ and are available upon request.

A. ${}^3\text{He}$

In Fig. 3, we present the data for the coexistence curve by a logarithmic plot $\Delta\rho/t^{0.32}$ vs $-t$. The exponent 0.32 represents the asymptotic number calculated from renormalization-group theory.¹² If the data were represented by a simple power law with this exponent, they would have to fall on a horizontal line. This type of plot was first used by Balzarini and Ohrn¹³ to expose in a sensitive way the dependence of β_{eff} on t . We note the continuous slope change indicating a decrease in β_{eff} as T_c is approached. The data closest to T_c are mainly those from the densities $\bar{\rho}/\rho_c = 0.982$ and 1.027 (liquid and vapor, respectively), while those beyond $t \approx 10^{-3}$ include also those for $\bar{\rho}/\rho_c = 1.00$. The systematic difference between the liquid and the vapor points for $t > 3 \times 10^{-2}$ is caused by the nonzero slope of the rectilinear diameter $\rho_d = \frac{1}{2}(\rho_L + \rho_V)$ that will be discussed below. Quite possibly, the low value of the vapor points

closest to T_c indicates that the meniscus has reached the bottom capacitor, and that a small fraction of the fluid between the plates is liquid.

The dependence of β_{eff} on the $|t|$ for $|t| > 8 \times 10^{-5}$ is presented in Fig. 4. It was obtained in two ways: First, from a fit of groups of, respectively, 15 and 25 neighboring density points (both liquid and vapor) to a simple power law. Successive groups were made to overlap by, respectively, 5 and 15 points. Second, from tracing a smooth line through the plotted points and taking the slope. For $t > 3 \times 10^{-2}$, the slope was obtained using the combination $(\rho_L - \rho_V)/2\rho_c = \frac{1}{2}\Delta\rho_{\text{liq.}} + \Delta\rho_{\text{vap.}}$. Two types of error bars are shown, reflecting, respectively, the standard deviation for the fits with the given choice of T_c (solid bars) and the uncertainty introduced by a $\delta T_c = \pm 30 \text{ } \mu\text{K}$ in the critical temperature (dashed bars). It is evident that in spite of the rapidly increasing uncertainty as $-t$ decreases, β_{eff} appears to tend to the asymptotic value predicted by theory. Also on this figure we show the curves for β_{eff} , had T_c been chosen 100 and 150 μK higher. For comparison, we show the results for β_{eff} reported by Stacey, Pass, and Carr⁸ and by Hayes and Carr⁷ for Xe. In the more recent work,⁷ the "quenching" method permitted an essentially gravity-free determination of the coexistence curve in the immediate proximity of T_c . The data of Thoën and Garland,⁹ not shown here for clarity, tend to $\beta_{\text{eff}} \approx 0.357$ for $|t| \geq 5 \times 10^{-3}$.

We now attempt a representation of $\Delta\rho$ in terms of a series of the type³⁰

$$\Delta\rho = |\rho_c - \rho_{L,V}| \rho_c^{-1} = B(-t)^\beta [1 + C(-t)^{\Delta'} + D(-t)^{2\Delta'} \dots] \quad (5)$$

Such a series has been suggested by theories that in-

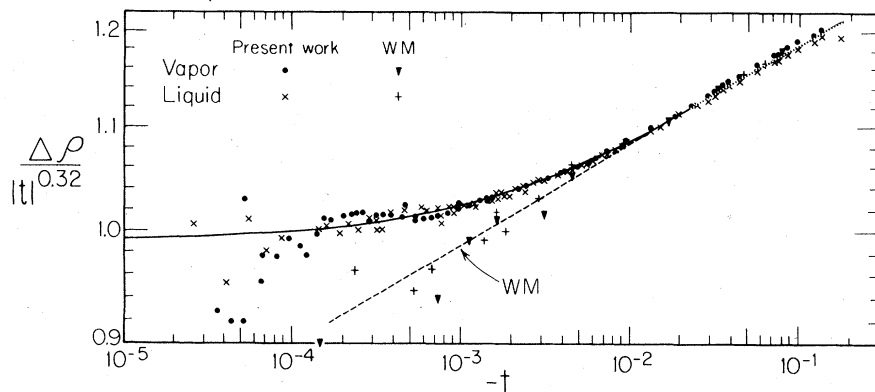


FIG. 3. Coexistence curve of ${}^3\text{He}$. Logarithmic plot of $\Delta\rho/|t|^{0.32}$ vs $|t|$ for both the liquid side (solid circles) and the vapor side (crosses). Here $\Delta\rho = (\rho_c - \rho_V)/\rho_c$ or $\Delta\rho = (\rho_L - \rho_c)/\rho_c$. The data were obtained for samples with several average densities $\bar{\rho}$. The systematic difference between the crosses and circles for $|t| \geq 3 \times 10^{-2}$ is caused by the nonzero slope of the rectilinear diameter. The solid line is the fit to Eq. (5) and the dotted line represents an average between liquid and vapor. The data by Wallace and Meyer (Ref. 2) that used an incorrect choice for T_c are shown for comparison. The dashed line corresponds to $\beta_{\text{eff}} = 0.360$.

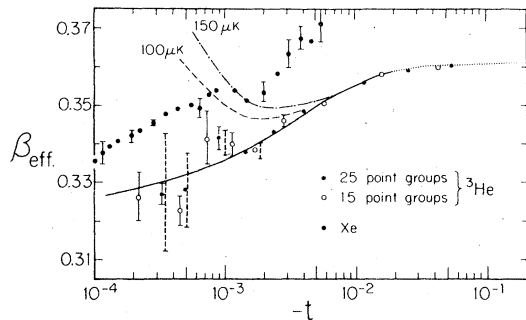


FIG. 4. Effective exponent β_{eff} , as defined by Eq. (1), obtained for ${}^3\text{He}$ from the coexistence curve data. The points were obtained by using a simple power law for groups of, respectively, 15 and 25 data points, with, respectively, 5 and 15 overlapping points between adjacent groups. The uncertainty expressed by solid error bars represents the standard deviation for such a simple power law. The dashed error bars represent the uncertainty in the determination of T_c , namely $\pm 30 \mu\text{K}$. For comparison, the data for Xe (Refs. 7 and 8) are also presented.

clude corrections to scaling. However, it appears that there are still uncertainties associated with such a representation.^{30,31} Accordingly we only present briefly our analysis, which may well be outdated by future theoretical expressions. Here we use again the individual liquid and vapor data for $-t < 3 \times 10^{-3}$,

while for $-t > 3 \times 10^{-3}$ the data are combined into $(\rho_L - \rho_V)/2\rho_c$, as above. As a first step in the fitting procedure, we used $\Delta' = 0.5$, based on the work quoted in Ref. 12 and left the other four parameters floating. We experimented with two routines. The first (R1) was a modification of a gradient search-type routine, while the second (R2) was CHIFIT taken from the book by Bevington.³² The results of these nonlinear fits are shown in Table III as a function of $|t|_{\text{max}}$, the maximum distance from T_c . Encouraged by the insignificant variation of β with $|t|_{\text{max}}$, we chose $\beta = 0.320$ as representative for the results up to $t = 4 \times 10^{-2}$ and obtained the amplitudes B , C , and D as a function of $|t|_{\text{max}}$, as shown in Table III. Our conclusion is that a two-term expression fits the data adequately up to $|t| = 1 \times 10^{-2}$. The amplitudes B and C from the three-term fit are in agreement with those from the two-term fit within the standard deviation up to $|t| \approx 1 \times 10^{-2}$. The three-term fit, adequate until approximately $|t| = 2 \times 10^{-2}$, is shown by the solid line in Fig. 3. This fit produces the β_{eff} shown by the solid line up to $|t| = 2 \times 10^{-2}$ in Fig. 4. Above this temperature, the dotted line in both figures represents the experimental curves. Figure 5 shows the deviation from the three-term linear least-squares fit, R3, up to $|t| = 2 \times 10^{-2}$. The quoted errors are from *statistics alone* and do not include the uncertainties in the choice of T_c .

TABLE III. The amplitude parameters for the power-law fit Eq. (5) as a function of the maximum temperature range $|t|_{\text{max}}$ and the number of data points over this range. The fitting program R1 is a modification of a gradient search-type routine, R2 is the CHIFIT routine (Ref. 30) and R3 is a linear fit. The numbers in parentheses were used as input.

$ t _{\text{max}}$	Number of points	β	B	C	D
R1					
5×10^{-3}	65	0.321 ± 0.006	1.000	0.939	0.259
1×10^{-2}	77	0.318 ± 0.004	0.966	1.418	-2.89
4×10^{-2}	85	0.321 ± 0.002	0.991	1.171	-1.91
1×10^{-1}	95	0.324 ± 0.002	1.025	0.911	-1.20
R2					
4×10^{-2}	85	0.322 ± 0.002	1.01	1.04	-1.51
R3					
2×10^{-3}	52	(0.320)	0.992 ± 0.002	0.847 ± 0.06	(0)
5×10^{-3}	65		0.991 ± 0.001	0.898 ± 0.02	(0)
1×10^{-2}	77		0.992 ± 0.008	0.877 ± 0.01	(0)
2×10^{-2}	81		0.995 ± 0.008	0.814 ± 0.01	(0)
1×10^{-1}	95		1.015 ± 0.02	0.552 ± 0.01	(0)
1×10^{-2}	77		0.990 ± 0.002	0.955 ± 0.07	-0.51 ± 0.47
2×10^{-2}	81		0.987 ± 0.001	1.06 ± 0.04	-1.25 ± 0.18
1×10^{-1}	95		0.988 ± 0.001	1.048 ± 0.01	-1.26 ± 0.02
R3					
		γ	Γ^+	E	F
2×10^{-2}	36	(1.240)	0.139 ± 0.003	3.19 ± 1.0	$-12. \pm 14.$

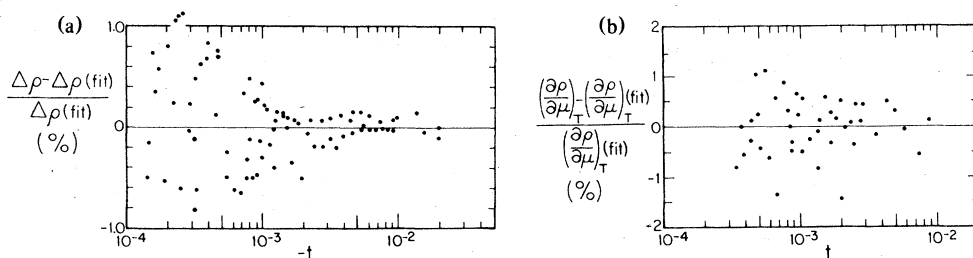


FIG. 5. (a) Percentile deviation from the three-term fit to the coexistence curve [Eq. (5)] using $\beta = 0.320$, $\Delta = 0.5$ over the range $|t| < 2 \times 10^{-2}$ (81 points). (b) The percentile deviation from the three-term fit to the compressibility data [Eq. (7)] with $\gamma = 1.24$, $\Delta = 0.5$ over the range $3 \times 10^{-4} < t < 2 \times 10^{-2}$.

In Fig. 6, the results above T_c are plotted as $(\rho_B - \rho_T)/\rho_c t^{-1.23}$ on the left scale and as the reduced compressibility $(P_c/\rho_c^2 t^{-1.23})(\partial\rho/\partial\mu)_T$ on the right-hand scale. The factor $t^{-1.23}$ is again used to produce a more sensitive representation and the chosen exponent is close to that expected from RG theory,¹² $\gamma = 1.24$. For $t > 5 \times 10^{-4}$, the points form a straight line with a slope of 0.04 ± 0.01 and the experimental data are represented by a simple power law

$$\frac{P_c}{\rho_c^2} \left(\frac{\partial\rho}{\partial\mu} \right)_T = \Gamma^+ t^{-\gamma_{\text{eff}}} = (0.209 \pm 0.015) t^{-1.19 \pm 0.01} \quad (6)$$

over more than two decades, with $P_c = 859.6$ Torr. For $t > 2 \times 10^{-2}$, $\delta\rho$ becomes small so that the scatter is large. The solid curve in Fig. 6 is calculated using the method of Hohenberg and Barmatz¹⁹ with the parameters given in Table II. From the agreement between the data and the curve, we conclude that for $t > 3 \times 10^{-4}$, where the departure from the linear vertical density profile is sufficiently small, the data are consistent with $\gamma_{\text{eff}} = 1.19$. The dashed curve in Fig. 6 represents our data corrected to simulate the

results for a very thin fluid sample. Below $t = 3 \times 10^{-4}$, the correction is too large to permit a reliable calculation of this curve. It is quite obvious that, unlike for the coexistence curve, our experimental conditions do not permit observing a clear deviation of the compressibility from a simple power law with an effective exponent γ_{eff} .

In spite of these limitations, we want to see whether our data are at least consistent with the limiting exponent γ predicted by theory and we fit the results for $t > 3 \times 10^{-4}$ to the expression

$$\frac{P_c}{\rho_c^2} \left(\frac{\partial\rho}{\partial\mu} \right)_T = \Gamma^+ t^{-\gamma} (1 + Et^{\Delta'} + Ft^{2\Delta'} \dots) \quad (7)$$

where the exponents are¹² $\gamma = 1.240$ and $\Delta' = 0.50$ and the amplitudes are left floating. Because the temperature range that could be used for the compressibility data analysis is appreciably smaller than that for the coexistence curve, only a fit with the total range is presented, and the parameters are presented in Table III.

We now check the relation among the critical amplitudes of the leading terms for the coexistence curve, the compressibility and the specific heat, the

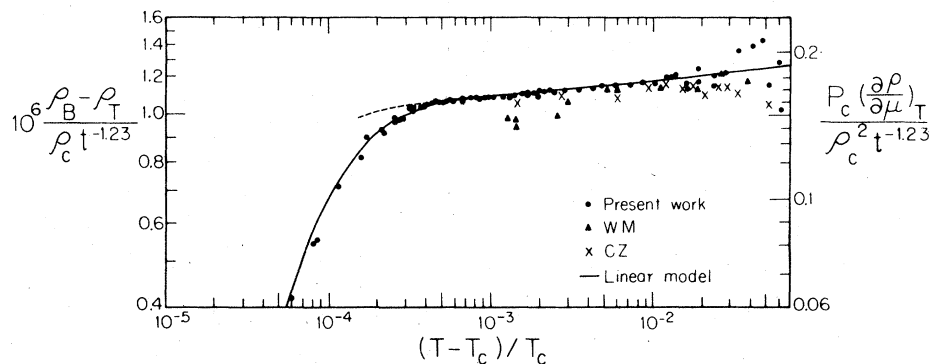


FIG. 6. Plot of $(\rho_B - \rho_T)/(\rho_c t^{-1.23})$ for ^3He vs t along the critical isochore (left-hand side scale). The dimensionless normalized compressibility $(P_c/\rho_c^2)(\partial\rho/\partial\mu)_T$ is the right-hand side scale. The solid line is calculated from the linear model using the parameters given in Table II.

latter two along the critical isochore. The calorimetric data,²⁴ transformed into dimensionless units, give

$$\frac{C_V T_c \rho_c}{P_c} = \frac{A^+ t^{-\alpha}}{\alpha} + C_B,$$

with

$$\left. \begin{aligned} \frac{A^+}{\alpha} &= 3.04, & C_B &= 0 \\ \alpha &= 0.11 \pm 0.01, \end{aligned} \right\} t < 10^{-2}. \quad (8)$$

The exponent α satisfies within the experimental uncertainty the scaling relation $\gamma + 2\beta = 2 - \alpha$ with $\gamma = 1.24$ and $\beta = 0.32$. From RG results, the predicted universal ratio is³³

$$\frac{A^+ \Gamma^+}{B^2} = 0.059 \quad (9a)$$

in reasonable agreement with the experimental value

$$\frac{A^+ \Gamma^+}{B^2} = 0.047 \pm 0.01. \quad (9b)$$

The greatest uncertainty in the experimental ratio is introduced by the uncertainty of about 10% in α . So far, no prediction for the ratios of the confluent singularity amplitudes such as E/C and F/D has been made. Such predictions would be highly desirable since they could be compared to experimental data on various fluids.

In Fig. 7, we show the linear diameter $\rho_d = \frac{1}{2}(\rho_V + \rho_L)$ vs $-t$ and the comparison with the data by Chase and Zimmermann,³ which are the most detailed ones taken previously. We deduce a slope

$$a = \rho_c^{-1} d\rho_d/dt = -0.022 \pm 0.002. \quad (10)$$

From an inspection of a for a number of fluids (see Table III of Ref. 24), we note that the sign becomes positive for ^4He and smoothly increases with T_c . This is shown in the insert of Fig. 7. Hence in this respect, ^3He is the fluid that is closest to the Ising model where $a = 0$.

We now discuss the new experimental results in relation to the earlier data of Refs. 2, 3, and 5. Figure 3 shows that for $|t| > 10^{-2}$, there is good agreement with the results by Wallace and Meyer.² But since in the earlier work, a simple power law was assumed, and the majority of the data were obtained for $|t| > 5 \times 10^{-3}$ and as far away as $|t| = 5 \times 10^{-2}$, it is not surprising that higher values for β were quoted, and the choice of T_c was probably incorrect. A too high value of T_c , respectively, raises and lowers the average value for β_{eff} and γ_{eff} obtained from a power-law fit (see Fig. 4) and therefore might well explain the values reported in Refs. 2 and 3 for $|t| < 10^{-3}$.

Turning to the compressibility, the amplitude in

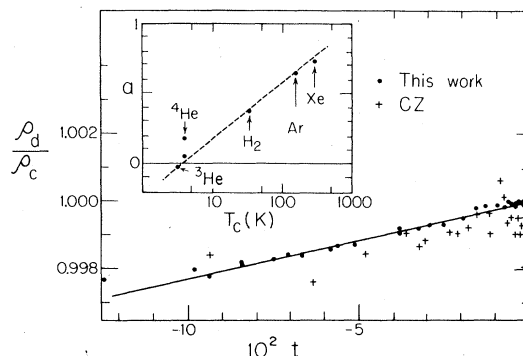


FIG. 7. Rectilinear diameter ρ_d for ^3He as a function of $-t$ and comparison with data by Chase and Zimmermann (CZ). Insert: the slope a of the rectilinear diameter for several gases as a function of their critical temperature T_c . The slopes for other fluids are given in Table I of the paper by M. R. Moldover and J. Gallagher, *Am. Inst. Chem. Eng.* **24**, 267 (1978). For SF_6 and CO_2 , the slope is, respectively, 0.86 and 0.99. The two points for ^4He mark the two determinations listed in Ref. 24.

Eq. (6) is in good agreement with the data of Refs. 2 and 3 presented in Table I. The data of earlier work are also shown in Fig. 5. The exponent deduced in Ref. 5 for $(\partial P/\partial T)_V$ data using the linear model was $\gamma = 1.16 \pm 0.02$ over the range $4 \times 10^{-4} \leq t \leq 6 \times 10^{-2}$ which is comparable with that in our new experiments. Hence, when a simple power-law analysis is used, there is reasonable consistency both in γ_{eff} and in the amplitude. For $T < T_c$, the compressibility exponent γ^- was derived from the jump of $(\partial P/\partial T)_\rho$ at the coexistence curve.⁵ Here a simple power-law analysis gave $\gamma_{\text{eff}}^- = 1.15 \pm 0.02$, while a fitting program to a leading term and a confluent singularity gives³⁴ an asymptotic $\gamma_{\text{eff}}^- = 1.17 \pm 0.02$.

It has been previously suggested^{5,35} that the temperature range, where the asymptotic exponents β and γ might be observed, is smaller for the He isotopes than for the heavier fluid such as Xe, which implies that the amplitudes of their correction terms C , D , etc. are larger. We have therefore sought to compare the results of the parameters in Eq. (5) with the corresponding ones⁷ in Xe. Recasting the three-term expression used by Hayes and Carr in their Table I, and using the parameters for points 1–38 ($|t| < 8 \times 10^{-3}$), we obtain the NMR frequency change Δf (in Hertz) that is proportional to $\Delta\rho$, namely,

$$\Delta f = 4381 |t|^{0.317} (1 + 3.05 |t|^{0.483} - 9.05 |t|^{0.933}), \quad (11)$$

where we have taken $T_c = 289.75$ K. The analysis by Ley-Koo and Green of the experimental data for SF_6 gives

$$\Delta\rho = 1.715 |t|^{0.327} (1 + 0.48 |t|^{0.49} - 0.84 |t|^{0.97}), \quad (12)$$

up to $|t| = 2.1 \times 10^{-2}$ with $T_c = 318.70$ K. The ex-

pressions for Xe and SF₆ are to be compared with the ^3He data for $|t|_{\text{max}} = 2 \times 10^{-2}$, where

$$\Delta\rho = 0.987|t|^{0.32}(1 + 1.06|t|^{0.50} - 1.25|t|^{1.00}) \quad (13)$$

If a new fit of the ^3He data is produced with the same exponents as in Ref. 7, our amplitudes merely change to $C = 1.3$ and $D = -1.9$.

It is quite obvious that the situation with respect to the correction-to-scaling amplitudes is confused; there is a large discrepancy between Xe and SF₆ that have nearly the same critical temperature, but the amplitudes for SF₆ and ^3He are quite comparable. From the latter evidence, we conclude that for ^3He , quantum effects³⁵ do not appear to shrink the asymptotic critical range, at least for the coexistence curve. Our experiments above T_c give only insufficient information on this point.

B. ^3He - ^4He mixture

In this section, we describe the data for the vertical density gradient $(\partial\rho/\partial Z)_T$ for the mixture with $X_3 = 0.80$ along the critical isochore.

The idea of our experiments results from the analysis of $(\partial\rho/\partial Z)_T$ in terms of thermodynamic properties. Let ρ be a function of the three fields T , P , and Δ . Then, at constant temperature

$$\left(\frac{\partial\rho}{\partial Z}\right)_T = \left(\frac{\partial\rho}{\partial P}\right)_{T,\Delta} \left(\frac{\partial P}{\partial Z}\right)_T + \left(\frac{\partial\rho}{\partial\Delta}\right)_{T,P} \left(\frac{\partial\Delta}{\partial Z}\right)_T \quad (14)$$

If we denote the average mass of the mixture by \bar{m} and the isotopic mass difference by δm , we obtain

$$\left(\frac{\partial\rho}{\partial Z}\right)_T = -g\rho^2 \left[\bar{m}k_{T,\Delta} + \delta m \left(\frac{\partial V}{\partial X}\right)_{T,P} \left(\frac{\partial X}{\partial\Delta}\right)_{P,T} \right] \quad (15)$$

where $k_{T,\Delta}$ is the isothermal compressibility at constant potential. A simple thermodynamic derivation leads to

$$k_{T,\Delta} = k_{T,X} + \frac{1}{V} \left(\frac{\partial V}{\partial X}\right)_{P,T}^2 \left(\frac{\partial X}{\partial\Delta}\right)_{P,T} \quad (16)$$

In not too diluted mixtures, $k_{T,X}$ is found to become roughly constant as T_c is approached^{27,28} and is predicted to diverge weakly immeasurably close to T_c .¹⁵ Also, calculations based on the model of Ref. 15 show that $(\partial V/\partial X)_{T,P}$ is a smooth function throughout the critical region. Therefore, it is concluded that $k_{T,\Delta}$ and $(\partial X/\partial\Delta)_{T,P}$ have the same divergence as T_c is approached. This is consistent with a derivation that uses a geometrical postulate by Griffiths and Wheeler,¹⁴ and predicts a strong divergence for both.

Finally,

$$\left(\frac{\partial\rho}{\partial Z}\right)_T = -\bar{m}g\rho^2 k_{T,X} - \left[\bar{m}\rho \left(\frac{\partial V}{\partial X}\right)_{P,T}^2 + \delta m \left(\frac{\partial V}{\partial X}\right)_{P,T} \right] \rho^2 g \left(\frac{\partial X}{\partial\Delta}\right)_{P,T} \quad (17)$$

Because the difference in the molar polarizability of ^3He and ^4He is negligible, the number density of the mixture can again be measured from the dielectric constant. Although $(\partial V/\partial X)_{P,T}$ has not been measured directly, it can be estimated from the relation

$$\frac{dV}{dX} = \left(\frac{\partial V}{\partial X}\right)_{P,T} + \left(\frac{\partial V}{\partial P}\right)_{T,X} \frac{dP}{dX} + \left(\frac{\partial V}{\partial T}\right)_{P,X} \frac{dT}{dX} \quad (18)$$

where the total derivatives are taken along the coexistence surface for the ^3He - ^4He mixtures; $(\partial V/\partial P)_{T,X}$ and $(\partial V/\partial T)_{P,X} = -(\partial V/\partial P)_{T,X}(\partial P/\partial T)_{V,X}$ can be calculated from existing data.^{34,35} This analysis gives $(\partial V/\partial X)_{P,T} = 990 \pm 100 \text{ cm}^3/\text{mole}$ for a point on the critical isochore of the $X = 0.80$ mixture at a temperature 5 mK above the critical point. Calculations from the Leung-Griffiths model¹⁵ for this mixture slightly above T_c yield $\sim 1050 \text{ cm}^3/\text{mole}$, in good agreement with the experimental value.

In Fig. 8, the $(\partial\rho/\partial Z)_T$ data for the mixture along the critical isochore $\rho_c = 0.0144 \text{ cm}^{-3}$ are presented in the form $(\partial\rho/\partial Z)t^{1.23}$ similar to Fig. 6. For comparison, the data for pure ^3He and ^4He are shown. The latter have been derived from the work of Roach and of Kierstead.¹ The dashed line denotes the calculated curve from the Leung-Griffiths model using Eq. (17). The error bar indicates an estimate of the systematic uncertainties resulting from the choice of the parameters. We draw attention to the relative magnitude of the terms in Eq. (17). Very close to T_c , the first term on the right-hand side is constant and is

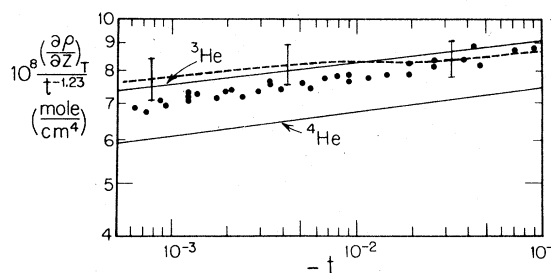


FIG. 8. Plot of $(\partial\rho/\partial Z)_T t^{1.23}$ vs t for the 80%- ^3He -20%- ^4He mixture (solid circles) and for pure ^3He and ^4He (solid lines) above the critical point and along the critical isochore. The dashed line is the calculated curve from the Leung-Griffiths model using the parameters selected by those authors.

small compared to the second one which diverges strongly. Far away from T_c (say for $t > 10^{-2}$) the term with $k_{T,X}$ diverges strongly and is comparable with the term in $(\partial X/\partial \Delta)_T$. Their sum does not yield a simple power law.

IV. SUMMARY

A. ^3He

We have carried out the most extensive series of measurements to date for densities of the coexisting liquid and vapor phases. The critical temperature T_c was located to within $\pm 30 \mu\text{K}$ using data at several densities close to the critical density ρ_c . The measurements extend over the range $3 \times 10^{-5} < |t| < 3 \times 10^{-1}$ where $t = (T - T_c)/T_c$. From measurements of the vertical density gradient $(\partial \rho/\partial z)_T$ in the earth's gravity field at densities close to ρ_c and above T_c , we determine the compressibility over the range $2 \times 10^{-2} > t > 3 \times 10^{-4}$.

Our main findings are: (i) The effective exponent β_{eff} describing the shape of the coexistence curve in the ρ - T plane decreases from a value 0.36 far from T_c and is consistent with an approach to the limiting value $\beta = 0.325$ predicted by theory for the lattice-gas model. The first value is in good agreement with previous results for ^3He and ^4He , while the second one is consistent with the findings for Xe, SF_6 , and CO_2 very close to T_c . (ii) The effective exponent describing the divergence of the compressibility at T_c is found to be $\gamma_{\text{eff}} = 1.19 \pm 0.01$ for $t > 3 \times 10^{-4}$ in agreement with previous results. For temperatures closer to T_c , the $(\partial \rho/\partial z)_T$ in the cell departs substantially from a constant value over the cell height and this prevents determining γ_{eff} sufficiently well. We have been, therefore, unable to see the expected increase of γ_{eff} to the limiting value of $\gamma = 1.24$. (iii) We have, however, been able to fit both the coexistence curve data as well as those for compressibility to expressions containing the asymptotic term (with exponents $\beta = 0.32$ and $\gamma = 1.24$) and correction-to-scaling terms. Together with the leading term from specific-heat data, an amplitude relation is obtained that is in fair agreement with that expected from theory. The amplitudes of the correction-to-scaling terms are comparable with those for SF_6 , indicating that the critical behavior of ^3He may not be different from that of heavier fluids. (iv) We have made a

substantially improved determination of the rectangular diameter slope a for ^3He . On a plot of the slope for pure fluids versus T_c , $a(^3\text{He})$ joins on smoothly to that of the other fluids. There is a change of sign for a between ^3He and ^4He .

B. ^3He - ^4He mixture

Here $(\partial \rho/\partial z)_T$ has been measured for a 80% ^3He -20% ^4He mixture above T_c . Plotted versus t , it is found to be intermediate between that measured for ^3He and that calculated for ^4He from compressibility data. Thermodynamic relations show $(\partial \rho/\partial z)_T$ to be proportional to the concentration susceptibility that is predicted to diverge strongly. This explains the observed strong divergence of $(\partial \rho/\partial z)_T$ in spite of the fact that for mixtures the compressibility at constant composition does not diverge strongly. Calculations of the $(\partial \rho/\partial z)_T$ from the Leung-Griffiths model for ^3He - ^4He mixtures are in good agreement with the experimental results.

We conclude this paper by noting that ^3He is of all the fluids the most susceptible one to gravity effects, as pointed out by Sengers¹² and also by Moldover *et al.*²⁰ Therefore, the determination of the effective critical exponents very close to T_c is a particularly difficult one, and cannot be carried out with the same accuracy as for Xe. A calculation furthermore shows that gravity effects for ^3He in an optical bending experiment⁶ will be at least as severe as in the capacitance method used here. At any rate, our results—at least for β_{eff} —remove the apparent discrepancy with the heavier fluids that was thought to exist very close to T_c .

ACKNOWLEDGMENTS

We thank Dr. P. Hohenberg for drawing our attention to the universal relations between critical amplitudes. Dr. M. R. Moldover made constructive comments on the manuscript and Professor R. B. Griffiths made a useful suggestion for an early calculation on the ^3He - ^4He mixtures. We also acknowledge a communication from Dr. H. Carr. This research was supported by a contract from the Air Force Office of Basic Research and a grant from the National Science Foundation.

*A preliminary analysis has been presented by the same authors in *Bull. Am. Phys. Soc.* **23**, 533 (1978).

†Present address: Natl. Bur. Stand., Gaithersburg, Md.

¹H. Kierstead, *Phys. Rev. A* **3**, 329 (1971); **2**, 242 (1973); and references therein to earlier work.

²B. A. Wallace and H. Meyer, *Phys. Rev. A* **2**, 1536, 1610 (1970). Tabulation of data: Technical Report, Duke University (1972) (unpublished).

³C. E. Chase and G. O. Zimmermann, *J. Low Temp. Phys.* **24**, 315 (1976).

- ⁴K. Ohbayashi and A. Ikushima, *J. Low Temp. Phys.* **19**, 449 (1975).
- ⁵R. P. Behringer, T. Doiron, and H. Meyer, *J. Low Temp. Phys.* **24**, 315 (1976).
- ⁶R. Hocken and M. R. Moldover, *Phys. Rev. Lett.* **37**, 29 (1976).
- ⁷C. E. Hayes and H. Y. Carr, *Phys. Rev. Lett.* **39**, 1558 (1977).
- ⁸L. M. Stacey, B. Pass, and H. Y. Carr, *Phys. Rev. Lett.* **23**, 1424 (1969).
- ⁹J. Thoen and C. Garland, *Phys. Rev. A* **10**, 1311 (1974); **13**, 1601 (1976); I. Smith, M. Giglio, and G. B. Benedek, *Phys. Rev. Lett.* **27**, 1556 (1971).
- ¹⁰A. B. Cornfeld and H. Y. Carr, *Phys. Rev. Lett.* **29**, 28 (1972).
- ¹¹W. T. Estler, R. Hocken, T. Charlton, and L. R. Wilcox, *Phys. Rev. A* **12**, 2118 (1975).
- ¹²Up-to-date reviews of critical phenomena in classical fluids including the most recent predictions by series expansion and renormalization-group theory are by J. V. Sengers and J. M. H. Levelt-Sengers, in *Progress in Liquid Physics*, edited by C. A. Croxton (Wiley, New York, 1978), p. 103; and by P. C. Hohenberg, in *Microscopic Structure and Dynamics of Liquids*, edited by J. Dupuy and A. J. Dianoux (Plenum, New York), p. 333.
- ¹³D. Balzarini and K. Ohrn, *Phys. Rev. Lett.* **29**, 840 (1972).
- ¹⁴R. B. Griffiths and J. C. Wheeler, *Phys. Rev. A* **2**, 1047 (1970).
- ¹⁵S. S. Leung and R. B. Griffiths, *Phys. Rev. A* **8**, 2670 (1973).
- ¹⁶See, for instance, C. J. F. Böttcher, *Theory of Electric Polarization* (Elsevier, Amsterdam, 1952).
- ¹⁷E. C. Kerr and R. H. Sherman, *J. Low Temp. Phys.* **3**, 451 (1970), and references therein.
- ¹⁸T. Doiron and H. Meyer, *Phys. Rev. B* **17**, 2141 (1978).
- ¹⁹P. C. Hohenberg and M. Barmatz, *Phys. Rev. A* **6**, 289 (1972).
- ²⁰M. R. Moldover, J. V. Sengers, R. W. Gammon, and R. J. Hocken, *Rev. Mod. Phys.* **51**, 79 (1979), have discussed in great detail the effects of gravity on the properties of fluids near T_c .
- ²¹L. A. Weber, *Phys. Rev. A* **2**, 2379 (1970).
- ²²M. G. Ryschkewitsch, T. Doiron, M. Chan, and H. Meyer, *Phys. Lett. A* **64**, 219 (1977); M. G. Ryschkewitsch and H. Meyer, *J. Low Temp. Phys.* **35**, 103 (1979).
- ²³M. Chan, M. G. Ryschkewitsch, and H. Meyer, *J. Low Temp. Phys.* **26**, 211 (1977).
- ²⁴G. R. Brown and H. Meyer, *Phys. Rev. A* **6**, 364 (1972).
- ²⁵G. R. Brown and H. Meyer, *Phys. Rev. A* **6**, 1578 (1972).
- ²⁶D. Dahl and M. R. Moldover, *Phys. Rev. A* **6**, 1915 (1972).
- ²⁷T. Doiron, R. P. Behringer, and H. Meyer, *J. Low Temp. Phys.* **24**, 345 (1976).
- ²⁸B. A. Wallace and H. Meyer, *Phys. Rev. A* **5**, 953 (1972).
- ²⁹See AIP document No. PAPS PRBMDO-20-3678-10 for 10 pages of supplementary tables. Order by PAPS number and journal reference from American Institute of Physics, Physics Auxiliary Publication Service, 335 East 45th Street, New York, N. Y. 10017. The price is \$1.50 for each microfiche (98 pages), or \$5 for photocopies of up to 30 pages with \$0.15 for each additional page over 30 pages. Airmail additional. Make checks payable to the American Institute of Physics. This material also appears in *Current Physics Microform*, the monthly microfilm edition of the complete set of journals published by AIP, on the frames immediately following this journal article.
- ³⁰M. Ley-Koo and M. S. Green, *Phys. Rev. A* **16**, 2483 (1977).
- ³¹T. S. Chang, C. W. Garland, and J. Thoen, *Phys. Rev. A* **16**, 446 (1977).
- ³²P. R. Bevington, *Data Reduction and Error Analysis for the Physical Sciences* (McGraw-Hill, New York, 1969).
- ³³A. Aharoni and P. C. Hohenberg, *Phys. Rev. B* **13**, 3081 (1976).
- ³⁴In actual fact, the analysis of the experiments in Ref. 5 gave the exponent combination $(\gamma + \beta - 1)\beta^{-1}$. A value of $\beta = 0.361$ was used to obtain γ . A choice of $\beta = 0.320$ would produce a still lower value of γ .
- ³⁵M. Suzuki, *Prog. Theor. Phys.* **56**, 1007 (1976).